Journal of Structural Geology, Vol. 10, No. 4, pp. 361 to 372, 1988
Printed in Great Britain

0191-8141/88 $03.00 + 0.00

Shear criteria in granite and migmatite deformed in the magmatic and solid states

PHILIPPE BLUMENFELD*

CREGU and GS CNRS-CREGU, BP 23, 54501 Vandoeuvre les Nancy Cédex, France

and

JEAN-LUC BOUCHEZ

Laboratoire de Pétrophysique et Tectonique, Université Paul Sabatier, 38 Rue des Trente-Six Ponts, 31400 Toulouse, France

(*Received* 27 *February* 1987; *accepted in revised form* 1 *December* 1987)

Abstract—Microstructural criteria for the determination of the sense of shear in rocks homogeneously deformed in the partially melted state are similar to those which apply to solid-state deformation. Sense of shear determination is either *direct*, deduced from the sense of rotation of markers, or *indirect*, involving the obliquity between the shear and foliation planes, or between the successive foliations imprinted at different stages of progressive deformation.

This study is a by-product of the detailed structural and microstructural investigation of a high-grade metamorphic rock pile (Variscan Vosges Massif, France) which underwent subhorizontal shearing during partial melting and further solidification. Depending on the rock chemistry, on the position in the pile and the relative timing of progressive deformation, layered migmatites and homogeneous granites were variously deformed in the partially melted and solid states. The sense of shear obtained from these rock types, using the criteria presented here, consistently gives a top to SW direction.

INTRODUCTION

IT IS now widely accepted that natural plastic deformation is mainly non-coaxial, simple shear being the simplest, and possibly also, the most representative model for these deformations. Non-coaxiality is expected in domains where deformation concentrates; for example, between crustal blocks moving past each other along surfaces that may be either vertical (e.g. transcurrent shear zones) or horizontal (flat-lying shear zones). Non-coaxial deformation is recorded in rocks by typical structures, which, once their formation is understood, are used by the geologist as 'shear criteria'. These criteria help to determine the sense of shear, and when the hypothesis of simple shear is demonstrated to be valid, may also help to estimate total strain (Ramsay 1980).

This paper concentrates on the determination of sense of shear in rocks deformed in the partially melted state. As in solid-state deformation, shear-sense determination is crucial for kinematic reconstructions in crustal sections where partial melting has occurred, and in syntectonic plutonic bodies. In the case studied here, non-coaxial deformation and sense of shear in a thick thrust pile of migmatites and granites has been documented both in the magmatic and solid states (Blumenfeld 1986). After discussing the criteria by which deformation in the magmatic state is distinguished from solid-state deformation, the geological setting of the thrust pile will be briefly presented. The principles supporting the determination of the sense of shear for the solid state will then be reviewed. Application of shear criteria to the partially melted state will be illustrated using four examples: (i) *C-S* obliquity between the shear plane and the magmatic foliation; (ii) obliquity between subfabrics; (iii) 'tiling' of megacrysts; and (iv) *S–S'* obliquity between composite foliations.

MAGMATIC VS SOLID-STATE DEFORMATION

Deformation of a magma leads to rotation and relative translation of the early-formed crystals embedded in the viscous matrix within which strain concentrates. If deformation in the partially melted state is followed by static crystallization, the shape-preferred orientation (SPO) of crystals, such as biotites and feldspars in a granite, is the unique memory of this deformation. The granite has a typical magmatic microstructure, mainly characterized by the euhedral habit of the early crystals, by growth fronts in feldspars, by an even distribution of the mineral species and a large size of the quartz crystals that, in addition, are free of intracrystalline strain features.

A subsequent solid-state deformation of the granite is easily recognized, at least under conditions of decreasing

* Present address: Department of Geology, University of Melbourne, Parkville 3052, Victoria, Australia.

temperature, using the intracrystalline features of quartz (Bouchez *et al.* 1981), the most ductile phase of quartzo-feldspathic rocks. Quartz aggregates readily elongate, recrystallize into smaller subgrains and new grains, and acquire typical lattice preferred orientations (LPO). At very high temperatures, especially under prograde metamorphism, the quartz grains may recrystallize due to grain-boundary migration. This may erase the optical deformation features. A closer inspection of the quartz grains is then needed in order to characterize the state of strain of their mineral inclusions. Presence of solid-state deformation in quartz prior to recrystallization is evidenced by the boudinage and kinking of these inclusions (Bouchez *et al.* 1984).

Both solid-state and magmatic deformations may be associated in migmatites. The gneissic structure, formed during deformation prior to partial melting, is characterized by anisotropic mineral-aggregate distributions due to deformation, and to anisotropic crystal growth possibly controlled by heterogeneous nucleation (McLellan 1983). This banding still remains in the mesosomes, the gneissic layers of the migmatites, where the crystalline skeleton was not destroyed during partial melting. On the contrary, the leucosomes, or granitic layers of the migmatites, which represent highly melted layers or masses of segregated liquid, acquire magmatic microstructures: the crystal distribution tends to randomize, and the grain size to increase in order to minimize surface energy (Johannes & Gupta 1982, McLellan 1983). Thus, an SPO of crystals in the leucosomes will be ascribed to deformation in the partially melted state.

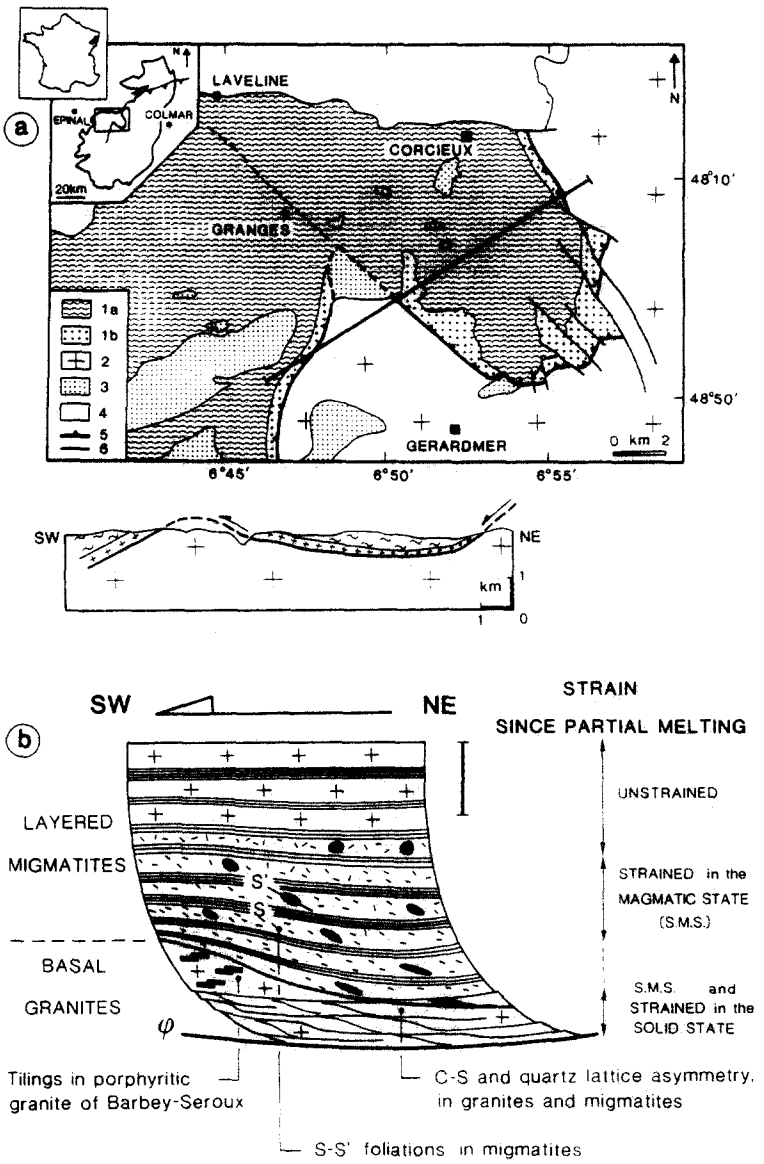

Fig. 1. (a) Geological sketch map and cross-section of the Variscan thrust pile in the Vosges massif (modified from Hameurt 1967). 1, Western Unit of the Central Vosges (a: Gerbépal migmatites, b: basal granitic sheet). 2, Axial Unit (granitic and gneissic formations). 3, Late intrusive and undeformed granitic bodies. 4, Unconformable Permian sandstones. 5, Thrust contact. 6, Fault. (b) Schematic and interpretative cross-section of the thrust pile that underwent subhorizontal shearing, in the solid state before partial melting, in the magmatic state, and again in the solid state after total crystallization. *Note* (1) The sense of shear towards SW within the migmatites and the granites deformed in the migmatic and/or solid-state; and (2) the strain gradient towards the base. The ellipses represent the cm-scale cordierite + quartz aggregates formed by liquid–biotite reactions during partial melting in the migmatites.

GEOLOGICAL SETTING

The thrust pile here considered is located north of Gérardmer, France (Fig. 1a), and has a thickness of several kilometres. It belongs to the Western Unit of the Central Vosges Massif (Hameurt 1967) which was thrust onto the Axial Unit during the Variscan orogeny (Blumenfeld 1986). The pile is mainly made of layered migmatites derived from partial melting at low pressure (350 MPa; cordierite–biotite association) of a volcano-sedimentary sequence metamorphosed under amphibolite-facies conditions (biotite, garnet and sillimanite). The base of the pile is a granitic sheet, varying in thickness up to a few hundreds of metres; it is layered in composition and grain size from fine to porphyritic. The compositions of the layers and the layering itself are thought to derive directly from the original composition of the layered gneisses forming the initial tectonic pile. Depending on the composition with respect to that of the granitoid eutectic, these layers produced various melt fractions during partial melting. Throughout the pile (Fig. 1b), the compositional layering of the migmatites and granite is roughly horizontal, parallel to the base of the pile. Within the migmatites, the residual metamorphic foliation, still preserved in layers having low degrees of melting, is also subhorizontal.

Whatever the position in the pile and the nature of the rock, a subhorizontal penetrative foliation and a constantly NE–SW-trending lineation is present (Fig. 2). The residual metamorphic fabric in many layers of the migmatite indicates that deformation pre-dated the onset of migmatization. The similarly oriented magmatic fabric recorded both in the migmatitic layers subjected to a high degree of melting, and in the granite sheet, argues that deformation continued after partial melting started. Because their initial fabric is mostly reset by partial melting, these latter rocks provide examples of shear criteria in the *magmatic state* (i, iii and iv). After total solidification, the imprint of solid-state deformation during decreasing temperature increases toward the base of the pile, as shown by stretching, recrystallization and LPO development in quartz (Blumenfeld *et al.* 1986). At the very base of the pile (0–300 m), especially in the northern part of the area (Fig. 1b), the orthogneissic structure overprints the granite, and locally the overlying migmatite; it is marked by the *C–S* composite planar association of Berthé *et al.* (1979).

The constantly oriented planar and linear structures of every type mentioned above, allied with the same sense of shear towards the south-west that is recorded throughout the pile in rocks deformed either in the solid or in the magmatic state (Fig. 1b), strongly support the conclusion of continuity in time of the same thrust event. Thrust-shearing first operated in the solid state in the high-grade metamorphic rocks and continued during partial melting. It progressively localized in the highly melted layers of the migmatites and in the granite, with a positive gradient toward the base of the pile. With decreasing temperature, thrust-shearing concentrated at the base of the pile, again in the solid state. Evidence for these interpretations are given below.

PRINCIPLES OF SHEAR CRITERIA

Sense of shear during non-coaxial deformation is obtained from the sense of rotation of the finite strain axes, deduced either directly from the rotation of individual grains (type 1), or indirectly from shape and lattice preferred orientations (type 2), which are related

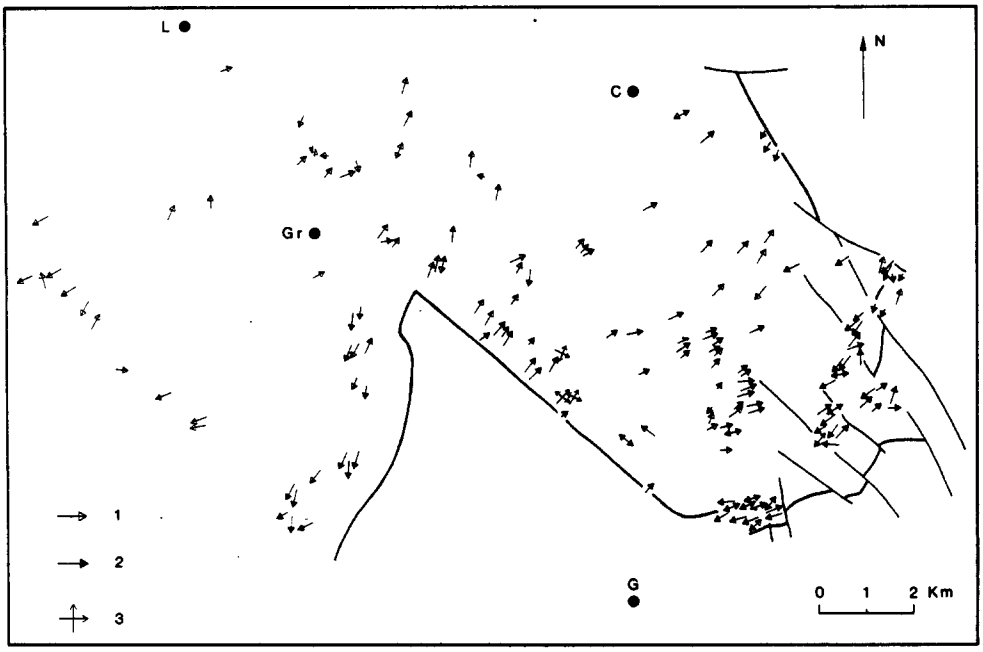

Fig. 2. Structural map of the stretching lineations in the migmatites and the basal granites of the western Vosges Unit. 1, Lineations on the foliation plane (*S*). 2, Lineations on the late shear plane (*C*). 3, Local subperpendicular set of lineations on the foliation plane of the porphyritic granite. Long arrow, gentle plunge; short arrow, steep plunge.

to the orientation of the finite strain axes. If reference is made to deformation in the solid state (Simpson & Schmid 1983), the direct (type 1) determination mainly refers to the rotation of porphyroblasts, evidenced by the snow-ball configuration of their inclusions (Schoneveld 1977) or of porphyroclasts with asymmetrical shadows and associated microfolds (Vernon 1987). Indirect determinations use the angular relationship either (type 2a) between the finite strain axes and the kinematic axes (or shear plane–shear direction frame) or (type 2b) between two sets of strain axes.

Indirect determination of the sense of shear requires the following definitions. The finite strain axes (X, Y and Z) are defined using the SPO of grains or aggregates: X is parallel to the average finite stretch, hence it is equated to L, the plastic lineation, and XY is parallel to the average flattening plane, equated to S, the foliation. The kinematic axes referred to in type 2a are defined using LPOs resulting from crystal-plastic deformation by dislocation creep (Bouchez *et al.* 1983): the shear plane (C) is considered as parallel to the average slip plane of grains, and the shear direction (L_s) as parallel to the average slip direction. For less penetrative deformation, for which strain tends to concentrate within parallel and regularly spaced shear bands, the shear bands are considered to be parallel to the shear plane (C) and the usually fine-grained aggregate lineation or striation they bear is considered to be parallel to the shear direction (L_s). In type 2b, the angular relationship between the two sets of strain axes refers to two generations of grains that have not recorded the same total strain. This occurs where a generation of new recrystallized grains continues deforming among older grains (Brunel 1980; Lister & Snoke 1984, Burg 1986).

The next section shows that the principles defined above also apply for the determination of the sense of shear in case of non-coaxial deformation in partially melted rocks.

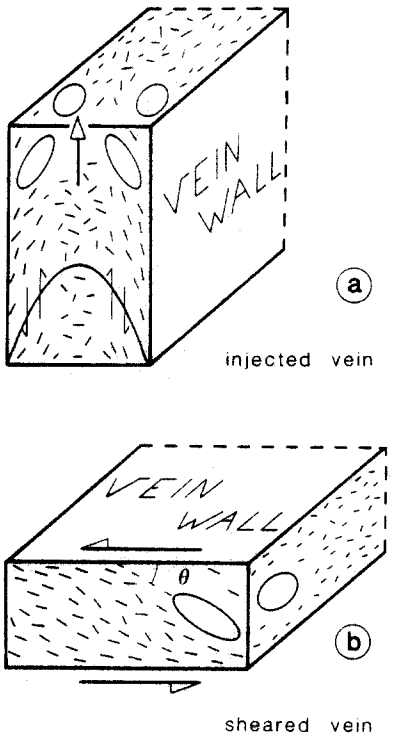

Fig. 3. Structures induced by magmatic shear in veins. (a) Finite strain and fabric of a magma injected between non-deforming walls. The curve shows the velocity profile across the vein for a Newtonian magma (from Johnson & Pollard 1973), with resulting opposite shear parallel to walls. Note the 'pinching' of crystals near the walls (from Blanchard *et al.* 1979), observed in the section perpendicular to the wall (shear plane) and parallel to the injection axis (shear direction), due to the symmetrically inclined finite strain ellipsoids. (b) Magmatic shear and finite strain pattern of a vein injected into an active fault. Foliation and lineation are oblique to walls at an angle θ. C–S obliquity indicates the sinistral relative movement of the vein walls.

SHEAR CRITERIA IN THE MAGMATIC STATE

'C–S' *obliquity*

If a magma contains a liquid fraction larger than the Rheological Critical Melt Percentage (RCMP of Arzi 1978; see also Van Der Molen & Paterson 1979, Fargier 1983), that is, more than 45% of liquid, free rotation of the anisotropic solid particles is allowed. Deformation induces a magmatic planar and linear crystal SPO during viscous simple shear. This fabric can be compared to the solid-state foliation and lineation described above if one invokes, for its development, the March (1932) model for which the whole material is considered to be continuous, the particles being ideal planes and lines. Hence, in the section parallel to the shear direction (L_s) and perpendicular to the shear plane (C), the angular relationship between the magmatic foliation plane (S) and the shear plane can be used as a shear sense criterion of type 2a. The fabric of granitic veins provides examples of such C–S obliquities.

A granite injected into *non-deforming* wall-rocks (Fig. 3a) undergoes opposite shear, parallel to the walls and symmetrically disposed about the medial plane of the vein (Johnson & Pollard 1973). This has been illustrated by Blanchard *et al.* (1979) who described the 'pincement' (pinching) of crystals at the vein-walls. It can be used as an indicator of the sense of injection.

If the granite is injected into an *active fault*, the magma may be sheared parallel to the walls, just as in a shear-box (Fig. 3b). Examples have been found in our thrust-pile, where fine-grained granite veins, a few centimetres in thickness, have been injected into early faults affecting the just solidified and still deforming porphyritic granite at the base of the pile (Fig. 1b). Progressive shearing of the veins, before and after the transition from magmatic to solid state, has been reconstructed using veins at various stages of total deformation. Such stages were recorded by different vein orientations with respect to the thrust geometry (Blumenfeld *et al.* 1985, 1986). Magmatic foliation and lineation of the least deformed veins are oblique to the walls by $\theta = 30°$ (Fig. 3b); the sense of shear given by the latter obliquity is the same as that given by the C–S association used for solid-state deformation. With decreasing θ values, a

plastic foliation–lineation develops; further deformation induces shear bands parallel to the walls, confirming that the walls indeed acted as shear planes. The unusual [c] direction of slip in quartz, with [c] parallel to the shear direction, has been documented from these granitic veins deformed under close to solidus and possibly hydrous conditions (Blumenfeld *et al.* 1986, Mainprice *et al.* 1986).

Obliquity between subfabrics

Rotation in a viscous matrix of rigid particles having various shapes has been studied by many authors (Gay 1966, 1968, Willis 1977, Ferguson 1979) on the basis of Jeffery's equations (1922). Due to the introduction of a shape parameter for the particles, these models depart from the March model in that the strain and fabric axes do not remain parallel to each other during non-coaxial deformation.

If two sets of particles with different n = length/width ratios are considered in a plane, two different *subfabrics* will appear, due to the different rates of rotation of the particles. The angular relationship between these subfabrics will give a criterion similar to type 2b for the determination of the sense of shear. This has been studied by Fernandez *et al.* (1983) using both numerical (Fig. 4a) and experimental (Fig. 4b) modelling of simple shear in two dimensions. A diagram (Fig. 4a) plotting the angle α, between the best axis of the fabric and the shear direction, vs the shear strain γ, shows that the thick particles (low n) rotate more rapidly toward shear plane ($\alpha = 0$) than the thin ones (high n); for large γ values, the thick particles depart more rapidly from the shear plane (α negative) than the thin ones. Hence the sign of $\Delta\alpha$ provides the sense of shear.

This method has been applied to the syntectonic granite of St. Sylvestre (France) by Lespinasse & Mollier (1985) using XY sections (perpendicular to magmatic foliation and parallel to lineation) of three different samples of known orientations with respect to the geographical frame. The $\Delta\alpha$ values for the subfabrics corresponding to the K-feldspar megacrysts (low n) and the biotites (high n) have the same sign for the three samples, varying from 8 to 29°. The resulting senses of shear are found to be compatible with each other. They also correlate with the sense of shear given by the tiling of the K-feldspar megacrysts, which is now discussed.

Tiling of megacrystals

Tiling of crystals refers to the imbrication of tiles in a roof (Fig. 6). It was first invoked by Den Tex (1969) to account for the oblique fabric of olivine crystals in ultramafic rocks. In porphyritic granite, tiling of K-feldspar megacrystals has been reported and interpreted (Blumenfeld, 1983) in the Barbey-Seroux granitic body cropping out at the base of the thrust pile (Fig. 1). In this granite, which is almost unaffected by solid-state deformation, the pervasive magmatic foliation (Fig. 6a) is marked by the SPO of the biotite, plagioclase and

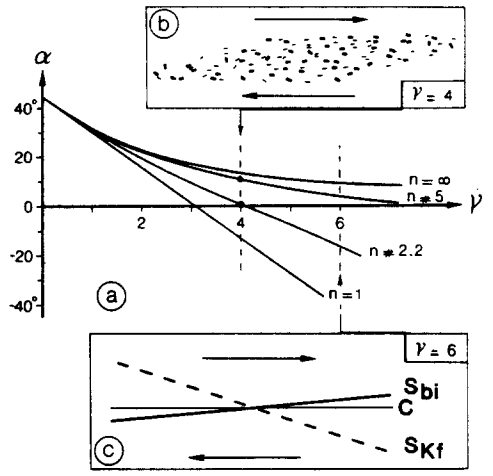

Fig. 4. Subfabrics in two-dimensional simple shear. (a) Calculated α angle, between the best axis of the fabric and the shear direction, vs shear strain γ, for different populations of rigid particles defined by their shape ratio (n = length/width; from Fernandez *et al.* 1983). $n = 1$: circular particle; $n = \infty$: linear particle. The curve for $n = \infty$ corresponds to the March model where $\alpha = \theta$, the angle between the finite stretch and shear direction. (b) Experimental model at $\gamma = 4$ of two subfabrics given by a mixture of thick ($n = 2.2$) and thin particles ($n = 5$). $\Delta\alpha$ is about 10°. The viscous matrix is a mixture of honey and titanium oxide, and the particles are made of PVC. From Fernandez *et al.* (1983). (c) A possible S–C pattern for high γ values in dextral shear that could be mistaken for sinistral. Magmatic fabric is oscillatory in increasing non-coaxial deformation (Willis 1977, Fernandez *et al.* 1983) and the period is a function of the particle shape ratio. The foliation S_{Kf} for thick particles (K-feldspars) overshoots the C position and tends to randomize. For thin particles (biotites—S_{bi}), this occurs only at very large strains ($\gamma > 7$). In that case (S_{bi}, L_{bi}) closely approximates to the March model.

K-feldspar crystals. Parallel to the foliation, the magmatic lineation is clearly defined using the average elongation and alignment of K-feldspars. Tiling of K-feldspar megacrysts is therefore a consequence of rotation in a viscous matrix, at least for a part of the population. It has been experimentally reproduced by Fernandez *et al.* (1983) with elongate rigid particles rotating in a viscous medium during simple shear, for γ values ranging from 3 to 5 (Fig. 6b).

If outcrops are examined in XZ sections (Fig. 6a), i.e. perpendicular to the planar structure and parallel to the linear one, individual examples of tiling reveal either a sinistral (Fig. 6c) or a dextral rotation (Fig. 6d) for a given couple (or group) of megacrysts. Statistical counting demonstrates that the population fraction giving a sense of tiling towards SW is of the order of 70% of the whole population (Fig. 5a). 50–400 tiling measurements per studied quarry are given in two columns in Fig. 5(a). The right-hand column gives the percentage of tilings rotating toward NE, and the left-hand one, towards SW. Hence, the number of rotations towards SW is consistently more than twice the number towards NE. This disproportion is more convincing if compared with counting performed along sections parallel to the magmatic foliation plane (XY section). The resulting percentage (Fig. 5b) of one sense of tiling with respect to the other, expressed by the deviation from 50% equipartition, is lower than 5% for 60% of the countings; it never exceeds 15% over more than 900 tiling measurements.

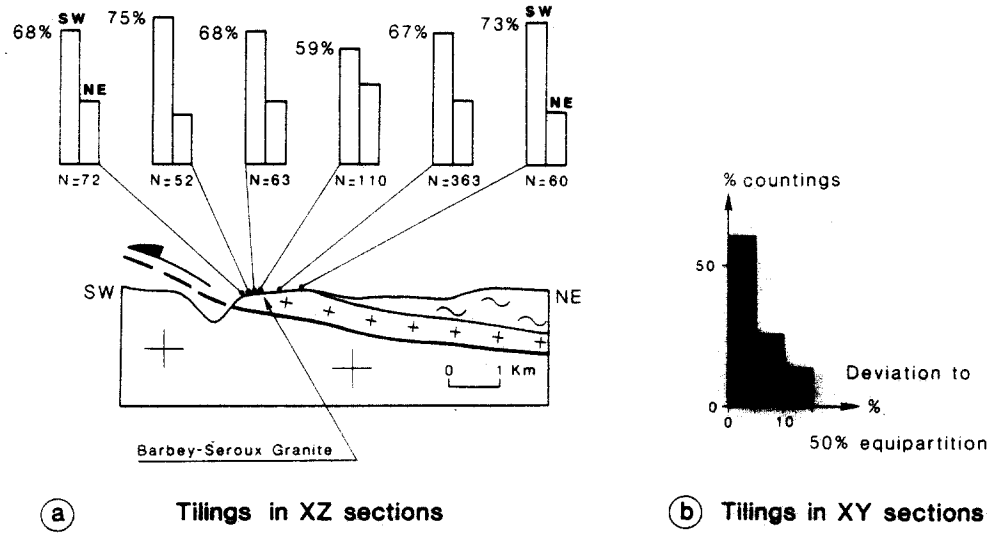

Fig. 5. Statistics of tilings in quarries of the Barbey-Seroux granite. (a) On surfaces parallel to the magmatic lineation and perpendicular to the magmatic foliation. Left-hand columns of histograms: percentage of tilings rotating towards SW; right-hand columns: towards NE. N = number of individual tiling features. (b) On surfaces parallel to the magmatic foliation, measured on one quarry. Frequency histogram of 23 different counting sets (911 individual measurements) giving the departure in measurement percentage from the equipartition with respect to the sense of tiling.

Statistical equipartition of the senses of tiling in the latter XY section is readily interpreted as due to the absence of a rotational component of strain in this section. This agrees with the rotation models for rigid particles in two-dimensional pure shear (Gay 1966, Blanchard *et al.* 1979) for which the two senses of rotation are equally represented. Conversely, the important deviation from equipartition in the XZ section supports the idea of non-coaxiality of deformation in that section. The dominant sense of rotation gives the sense of shear (type 1 criterion). Departure from the theoretical models of simple shear in two-dimensions (Jeffery 1922, Willis 1977, Fernandez *et al.* 1983) for which every particle rotates in the same sense, may be explained in two ways.

(1) Strain in the pile departs from simple shear. This is supported by the shape ellipsoids of quartz + cordierite aggregates measured in the overlying migmatites. If these markers do represent the ellipsoid of finite strain undergone since their formation, they variously depart from plane strain, mainly into the flattening field, with average k values (Flinn 1962) of 0.70 (Blumenfeld 1986).

(2) Contrary to numerical models where the particles are supposed to be totally interaction-free (high dilution hypothesis), interactions do occur among K-feldspars, increasing with their concentration, and with strain for a given concentration. These interactions result from rotation, but also from relative translation of crystals, which become closer to each other along the shortening axis (Z). Hence, some tiling features do not exclusively result from rotation. This may explain tilings giving the opposite sense of rotation.

This criterion enables us to rule out emplacement of the Barbey-Seroux granite sheet as a late laccolith, since shearing of the granite is consistently top towards SW from the top to the base of the sheet (Fig. 5a). Evidence for the sense of shear is now presented using another criterion in the migmatites.

S–S′ *foliations in the migmatites*

The migmatites of the pile are composed of successive layers, a few millimetres to a metre in thickness, which locally are cross-cut by cm-thick dykelets that collected magma from the most melted layers. The variable degree of partial melting in the different layers is mainly controlled by the variable initial composition (Blumenfeld 1986). Melt fraction (%F) of a given layer at a given temperature has been computed from the calculated modal composition, using the data of the haplogranitic system at constant water pressure. Thus, for a given temperature, a layer having a *gneissic structure*, that is, a well-preserved banded structure, usually has a lower %F than a layer having a *granitic structure* (Fig. 8). This is mainly due to the plagioclase composition, which is richer in anorthite, by 5 wt% on average, in the gneissic layers than in the granitic ones. Hence fusion in the gneissic layers starts at slightly higher temperature than in the granitic layers. Considering now the steep slopes of the %F vs temperature curves at the onset of melting (Fig. 8), and concentrating on the realistic domain of 0–50% for %F in migmatites, the difference in melt fractions between the two layers is about 20%. Depending upon modal compositions and experimental data chosen for the calculation, differences in %F range from less than 10% to 40%.

In the *gneissic* layers, the residual metamorphic foliation (S) is parallel to the biotite (001) cleavage preferred orientation (Fig. 9b). It is also parallel to mm-thick laminae alternatively enriched in biotite + plagioclase and in quartz + K-feldspar. A clearly defined mineral and aggregate lineation (L) is present. In contrast, the

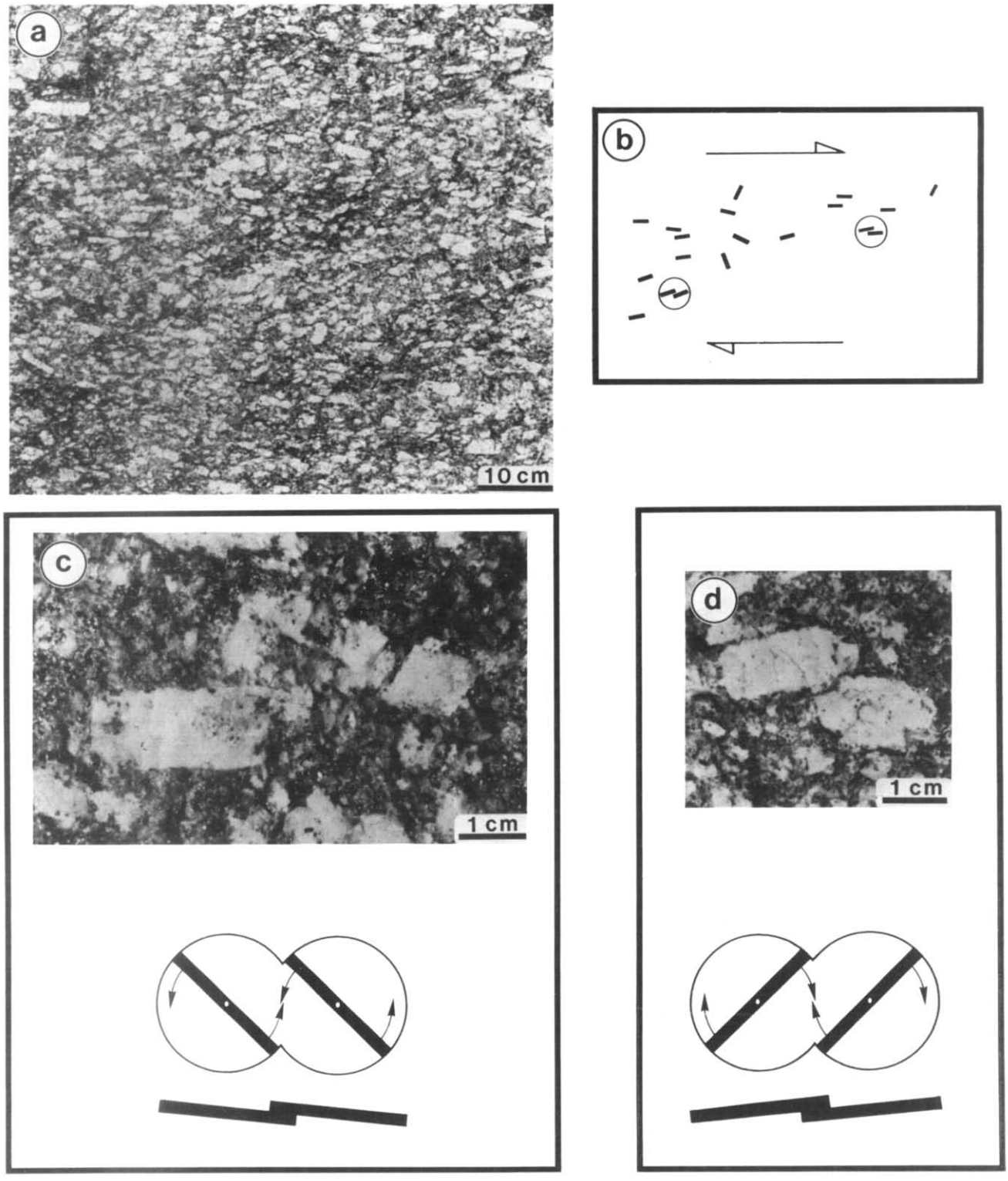

Fig. 6. The tiling of crystals. (a) The Barbey-Seroux granite (see Fig. 1). Well defined fabric of K-feldspar megacrystals in section perpendicular to the magmatic foliation and parallel to lineation. (b) Dextral simple shear experiment of a viscous matrix containing rigid particles (from Fernandez *et al.* 1983), giving dextral tiling features (circled). (c) and (d) Sinistral and dextral tiling of K-feldspar megacrysts in the Barbey-Seroux granite, respectively.

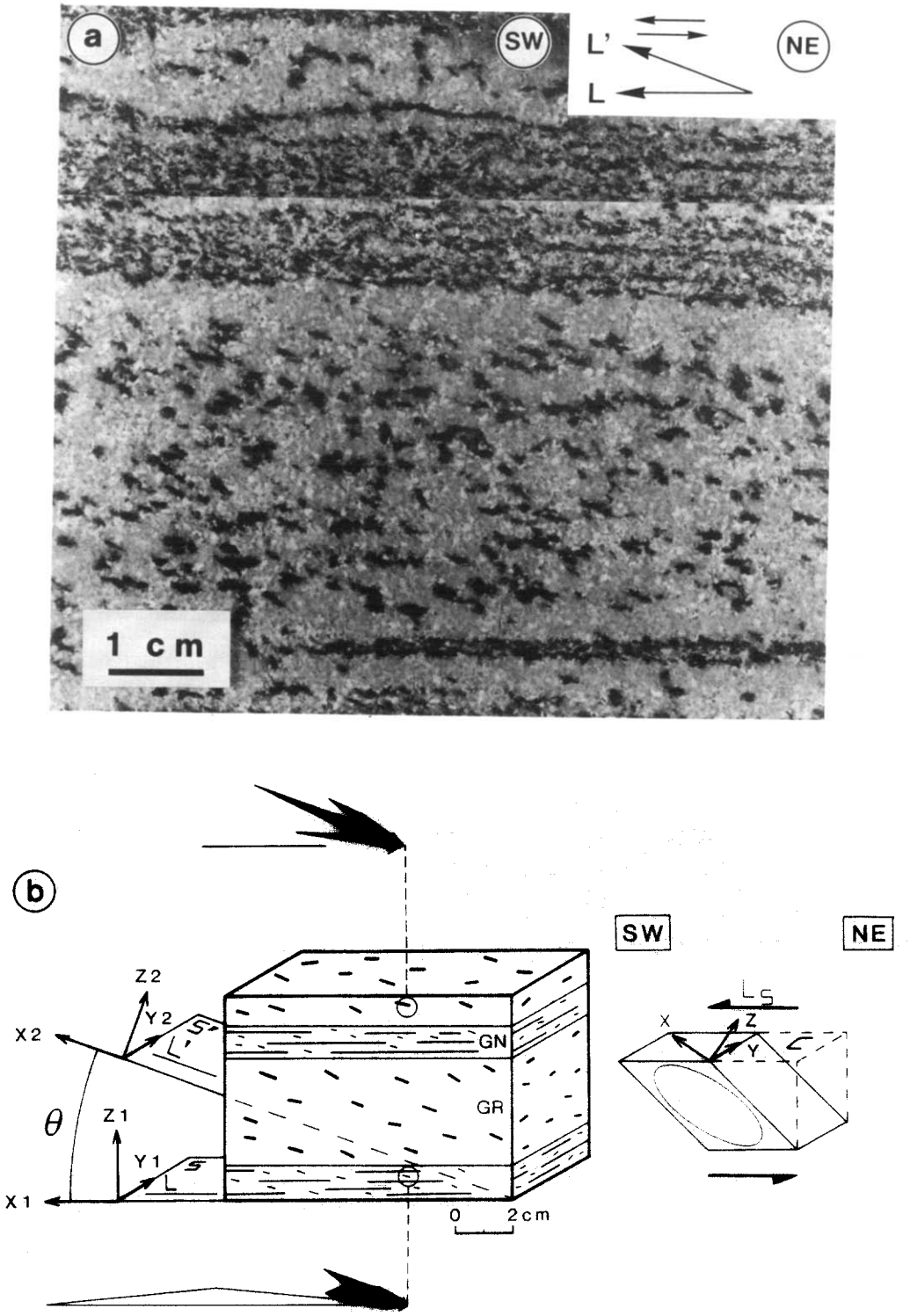

Fig. 7. S–S' obliquity in a migmatite (outcrop M44; see Fig. 10). View of an XZ section (a), and corresponding block-diagram (b), illustrating the relationship between (S,L) and (S',L). Alternating granite layers (GR) with ellipsoidal (S',L') clusters of biotite, and gneissic layers (GN), with an intermediate structure consisting of residual metamorphic banding (S,L) with or without scattered individual biotite crystals. Note that (S',L') can be defined either on the biotite clusters of the GR layers, or on the scattered biotites of the GN layers. Rose diagrams: XZ sections; filled in black for traces of S'; unfilled for trace of residual S. A SW-directed shear explains the old, total finite (S,L) frame, indicated by (X_1, Y_1, Z_1), as well as the more recent partial finite (S',L') frame (X_2, Y_2, Z_2).

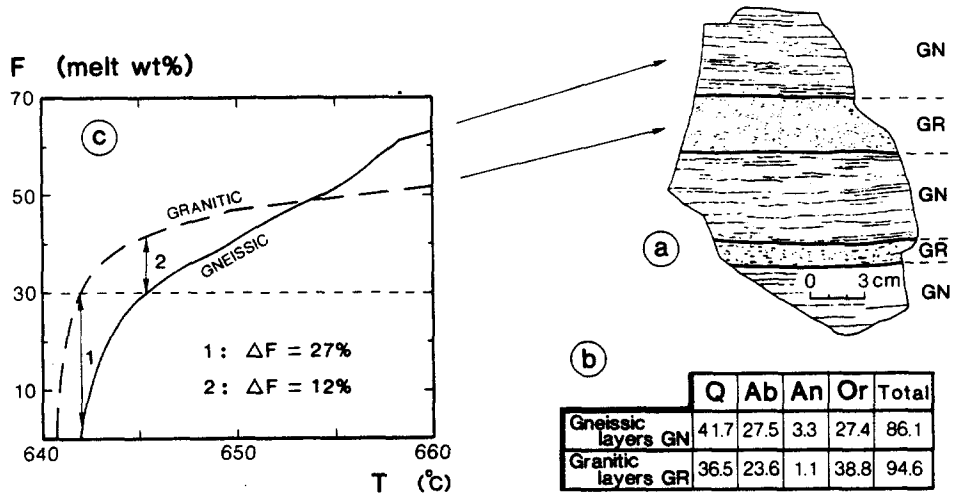

	Q	Ab	An	Or	Total
Gneissic layers GN	41.7	27.5	3.3	27.4	86.1
Granitic layers GR	36.5	23.6	1.1	38.8	94.6

Fig. 8. Partial melting of the layered migmatite (Arrentès-de-Corcieux quarry; outcrop 41 of Blumenfeld 1986; high level in the pile). (a) Typical migmatite with alternating gneissic (GN) and granitic (GR) layers, inherited from layers of the original volcano-sedimentary series. *XZ* section. (b) Modal compositions of the layers, computed from the average chemical analyses. Q, quartz; Ab, albite; An, anorthite; Or, orthoclase; Total, quartzo-feldspathic fraction of the rocks. (c) Computed melt weight percentage (F) vs temperature for the two types of layer, using the experimental data of the haplogranitic (Q, Ab, An, Or) system at $PH_2O = P_T = 5$ kbar (Winkler 1979).

granite layers do not display any compositional laminae, and the biotite crystals are homogeneously distributed, either as scattered individuals or as ellipsoidal biotite + quartz clusters (Fig. 7a). Where biotite is scattered throughout the granite layers, its (001) cleavage preferred orientation, although less pronounced than in the gneissic layers, reveals an average planar disposition S' which is oblique with respect to S by about 20° (Fig. 9c). The zone axis of this disposition, which is normal to the girdle of the (001) poles, always indicates an L' lineation the projection of which onto the S plane is parallel to L of the gneissic layers (Fig. 9c). The average flattening plane (S') and elongation direction (L') of the biotite clusters have the same geometry (Fig. 7).

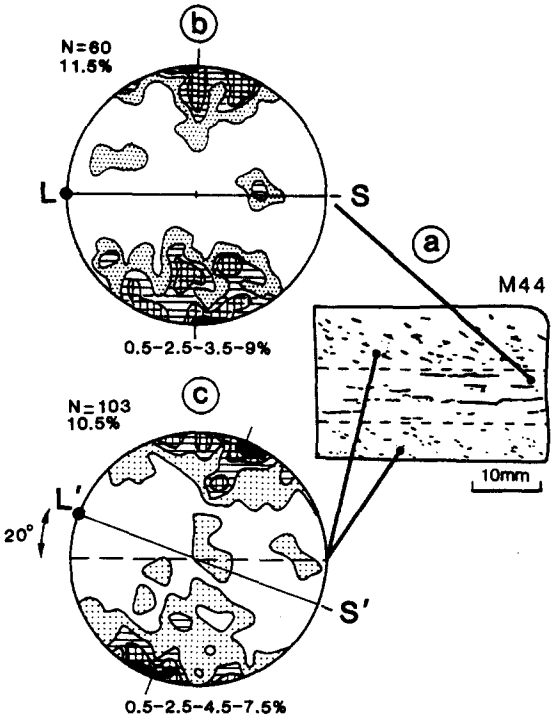

Fig. 9. Preferred orientation patterns of biotite in gneissic (b) and granitic (c) layers of the migmatite (a). (a) Sketch from a thin-section showing a central gneissic layer, with residual metamorphic banding, bordered by two granitic layers with scattered biotites. (*XZ* section, outcrop M44, located in Fig. 10). (b) and (c) Poles to biotite (001) cleavage planes in the gneissic (b) and the granitic (c) layers. U-stage measurements; lower hemisphere equal-area projections; labels: contours per 1% area, number of measurements (N) and maximum density. L–L' : lineations; S–S' : trace of foliations.

The initial gneissic fabric (S,L) progressively disappears when %F exceeds about 30%, leading to a reset of the 'finite strain clock' (Lister & Snoke 1984). The obliquity between the (S,L) fabric of a gneissic layer and the (S',L') fabric of a 'reset' layer is therefore ascribed to the differences in the recorded finite strains during the same non-coaxial deformation event (Fig. 7b). In other words, the (S,L) fabric of a gneissic layer, which is always very pronounced, has recorded the total shear strain undergone by this specific layer, whereas the (S',L') fabric of a granitic layer has only recorded the shear strain increments that were added since partial melting attained about 30% of liquid.

The obliquity between S and S' has been systematically observed and reported in the form of rose-diagrams over regularly distributed outcrops of the thrust pile (Fig. 10): it is always compatible with a SW-directed shear. It constitutes a criterion of type 2b for non-coaxial deformation and sense of shear in migmatites.

These S–S' foliations demonstrate that horizontal-shearing of the pile started before the onset of partial melting. In addition, the increasing stretching and flattening of the cordierite + quartz ellipsoids toward the base of the magmatites shows that total strain recorded in the partially melted state increased from the top to the base of the pile (Fig. 1b and caption). At the base, the calculated γ due to magmatic shearing may attain 2. At the very base of the pile, the magmatic S–S' structure is progressively overprinted by an orthogneissic C–S structure, characteristic of solid-state deformation, which also indicates a SW-directed shear. The latter demon-

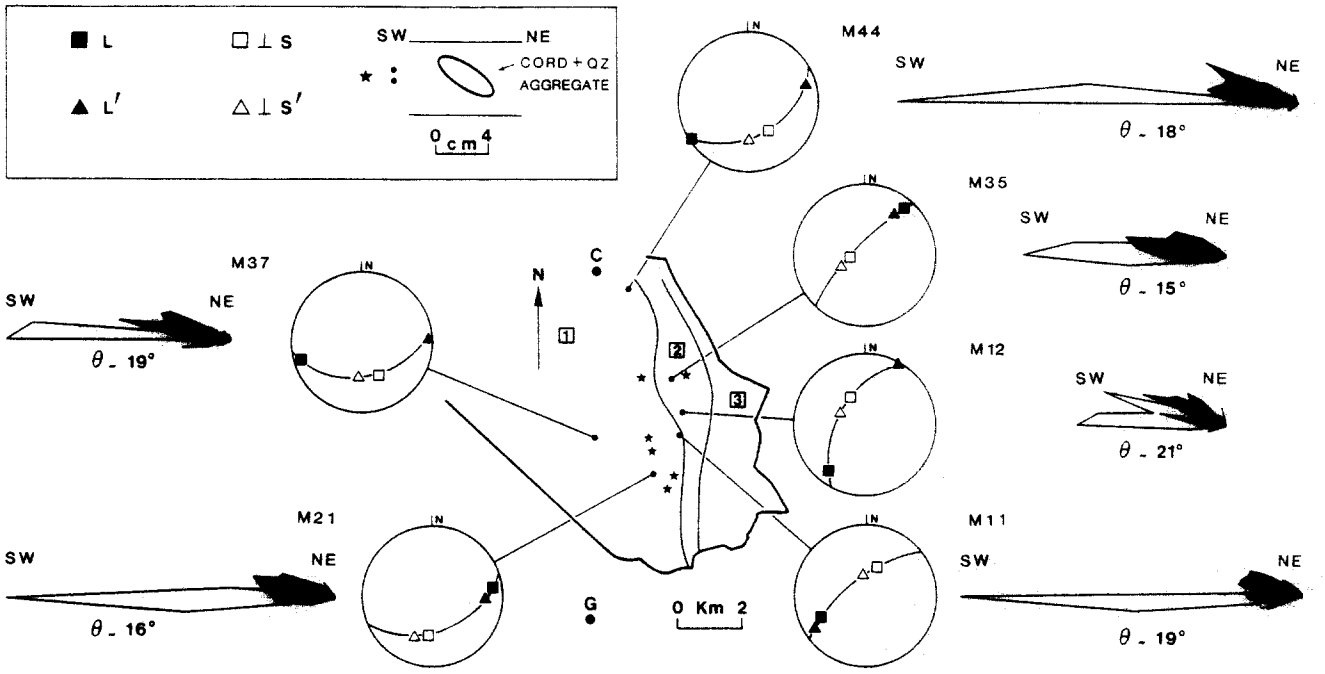

Fig. 10. *S–S'* obliquities in the migmatites. Map of the Western Unit—*zone 1*: no solid-state deformation in the granitic layers of the migmatite and in the granite sheet (round quartz aggregates); *zone* 2: homogeneous and moderate solid-state deformation; *zone* 3: heterogeneous deformation and presence of *C* planes. Stars: sites where ellipsoidal cordierite + quartz aggregates are oblique with respect to the residual banded structure (S, L). Six outcrops are detailed with stereograms of (S, L) and (S', L') determined on oriented samples and rose diagrams of preferred orientations (XZ section) of the residual banded structure (S, L: unfilled; 15–75 measurements) and of the scattered biotites (S', L: full; 130–160 measurements). $\theta = (S \wedge S') \simeq (C \wedge S')$ is determined from the rose diagrams.

strates that deformation was progressively localized at the base of the pile, and that thrust-shearing ended after total crystallization of the rocks.

DISCUSSION AND CONCLUSION

In this high-grade metamorphic pile deformed by horizontal shearing during the Variscan orogeny, the SW-directed sense of shear is identified using the shear criteria that have been progressively demonstrated during the last decade for solid-state deformation. The same basic principles are here shown also to apply to rocks deformed in a partially melted state. In these rocks, identification of shear during partial melting is obviously impeded if the magmatic structure is overprinted by other structures due to subsequent deformations. This arises in the lower portion of the pile (Fig. 1b).

When the melt fraction is high enough to minimize particle interactions during deformation, the average planar and linear disposition of the particles respectively represent the finite-flattening plane (S) and stretching axis (L), if the March model is applied. This is represented in two dimensions by the curve $n = \infty$ of Fig. 4(a). The biotite crystals closely approximate the latter condition ($S_{bi} = S$; $L_{bi} = L$) up to very high strains. Particles with lower aspect ratios, namely K-feldspars ($n = 2$–3), have S_{Kf} and L_{Kf} departing from the finite S and L framework. Hence, the sense of shear determination directly results from the C–S_{bi} obliquity (in sections perpendicular to S and parallel to L) provided that the shear plane (C) is known by other means. This is the *C–S obliquity criterion*, here applied to veins where shear is parallel to the walls. This is also true for the C-S_{Kf} obliquity, provided that γ remains low enough (say <4; Fig. 4a). For high γ values, say >5, corresponding to about half a fabric-cycle in the sense of Fernandez *et al.* (1983), the S_{Kf} plane may overshoot the position of the C plane. This may lead to a misinterpretation of the sense of shear (discussed in Fig. 4c). Note that the fabric of the K-feldspars should also become disorganized at that stage.

If distinct subsets of particles are considered, the obliquity between planar subfabrics, such as S_{bi} and S_{Kf}, based on the different vorticities of the particles as a function of their elongation, can be regarded as a criterion of the sense of shear. In practice, one must work on saw-cut rock-sections properly oriented perpendicular to S and parallel to L.

When the melt fraction of the granite reduces toward the Rheological Critical Melt Percentage for which the magma becomes rigid, particle interactions increase, along with their tendency to pile-up during rotation, giving the *tiling* criterion.

The syntectonic migmatites are characterized by layers that contained different melt fractions during deformation. In thick layers (>10 cm) with large melt fractions (≫RCMP) the criteria defined for granites may apply. For moderate melt fractions around the RCMP, some (gneissic) layers keep their early (S,L) fabric acquired during solid-state deformation whereas others (granitic) have fabrics that randomize at higher melt fractions. If the shear strain added after fusion remains limited, any new (S', L') structure imprinted on a granitic layer will record a finite strain that is less intense than that given by the (S,L) structure of a neighbouring

gneissic layer. The resulting obliquity between S and S' constitutes a shear criterion for migmatites. However, if shear added after fusion is large ($\gamma > 5$), S' may overshoot the position of C, and hence necessarily overshoot that of S. This may result in an inversion of the S–S' obliquity (Fig. 4c). In the migmatites discussed here, shear flow in the magmatic state was moderate in intensity ($\gamma \simeq 2$) such that (S_{bi}, L_{bi}) remained approximately parallel to (S,L). This is consistent with the long axis orientations of the cordierite + quartz and biotite + quartz ellipsoids present in layers with high melt fractions (Figs. 1b and 7).

As temperature decreases, and disregarding the peculiar structures that may be imprinted on the rocks during the transient state just before total solidification (Bouchez & Guineberteau in press), the rock enters the domain of fabrics due to *solid-state deformation*, for which shear criteria are well established. Hence, and in spite of some departure from the finite strain frame in specific cases (see above), this study shows that the S plane and L line formed in the partially melted state can be considered to be parallel to the finite flattening plane and stretching direction, just as for solid-state deformation (Nicolas & Poirier 1976, Ramsay 1980), in which various mechanisms lead to progressive rock flattening and stretching during shear. We therefore propose to use the terms foliation (S) and lineation (L) for both the partially melted and the solid-states, with qualification as to magmatic or solid-state, depending on the physical state of the rock during the deformation which produced the structure.

In conclusion, with the help of a Variscan thrust pile deformed both in the magmatic and the solid states, shear criteria for solid-state deformation have been extended to the magmatic deformation. Everywhere in the pile these criteria demonstrate subhorizontal shearing towards SW. With a view to kinematic reconstructions of basement rocks, we emphasize that partially melted rocks and their associated magmatic bodies are potential markers that must not be neglected.

Acknowledgements—The Centre de Recherches sur la Géologie de l'Uranium (CREGU) of Nancy and the Laboratoire de Tectonophysique of the University of Nantes (UA CNRS 732) are acknowledged for their support. Claude Gagny, Professor at the University of Nancy, initiated this work. Michel Cuney (CREGU) and Bernard Poty (Director of CREGU) encouraged us during the work. David Mainprice of the University of Montpellier and Ron Vernon of Macquarie University offered us many helpful suggestions that have improved the paper. Support in Toulouse University was kindly offered by Jean-Pierre Bouillin (UA CNRS 145) and Jean-Pol Fortuné (UA CNRS 67).

REFERENCES

Arzi, A. A. 1978. Critical phenomena in the rheology of partially melted rocks. *Tectonophysics* **44**, 173–184.

Berthé, D., Choukroune, P. & Jegouzo, P. 1979. Orthogneiss, mylonite and non-coaxial deformation of granites: the example of the South Armorican Shear Zone. *J. Struct. Geol.* **1**, 31–42.

Blanchard, J. P., Boyer, P. & Gagny, C. 1979. Un nouveau critère de sens de mise en place dans une caisse filonienne: le 'pincement' des minéraux aux épontes. *Tectonophysics* **53**, 1–25.

Blumenfeld, P. 1983. Le 'tuilage des mégacristaux', un critère d'écoulement rotationnel pour les fluidalités des roches magmatiques. Application au granite de Barbey-Seroux (Vosges–France). *Bull. Soc. géol. Fr.*, 7 *Ser.* **XXV**, 309–318.

Blumenfeld, P. 1986. Déformation et fusion partielle dans la croûte continentale. Migmatites et granites de l'Unité Occidentale des Vosges moyennes (France). Unpublished thesis, Université de Nancy, France.

Blumenfeld, P., Mainprice, D. & Bouchez, J.-L. 1985. Glissement de direction [c] dominant dans le quartz de filons de granite, cisaillés en conditions sub-solidus (Vosges–France). *C.r. hebd. Séanc. Acad. Sci., Paris* **301**, 1303–1308.

Blumenfeld, P., Mainprice, D. & Bouchez, J.-L. 1986. *C*-slip in quartz from subsolidus deformed granite. *Tectonophysics* **127**, 97–115.

Bouchez, J.-L., Guillet, P. & Chevalier, F. 1981. Structures d'écoulement liées à la mise en place du granite de Guérande (Loire-Atlantique, France). *Bull. Soc. géol. Fr.*, 7 *Ser* **XXIII**, 387–399.

Bouchez, J.-L. & Guineberteau, B. Écoulement dans les granitoïdes: de l'état visqueux à l'état solide. *Géol. Géochim. Uranium, Mém. Nancy*. In press.

Bouchez, J.-L., Lister, G. S. & Nicolas, A. 1983. Fabric asymmetry and shear sense in movement zones. *Geol. Rdsch.* **72**, 401–419.

Bouchez, J.-L., Mainprice, D. H., Trépied, L. & Doukhan, J. C. 1984. Secondary lineation in a high-T quartzite (Galicia, Spain): an explanation for an abnormal fabric. *J. Struct. Geol.* **6**, 159–165.

Brunel, M. 1980. Quartz fabrics in shear-zone mylonites: evidence for a major imprint due to late strain increments. *Tectonophysics* **64**, 33–44.

Burg, J. P. 1986. Quartz shape fabric variations and *c*-axis fabrics in a ribbon-mylonite: arguments for an oscillating foliation. *J. Struct. Geol.* **8**, 123–131.

Den Tex, E. 1969. Origin of ultramafic rocks. Their tectonic setting and history. *Tectonophysics* **7**, 457–488.

Fargier, L. 1983. Étude expérimentale de la transition dynamique liquide–solide sur des particules de paraffine en suspension dans un liquide. Unpublished DEA, Université de Nantes, France.

Ferguson, C. C. 1979. Rotations of elongate rigid particles in slow non-newtonian flows. *Tectonophysics* **60**, 247–262.

Fernandez, A., Feybesse, J. L. & Mezure, J. F. 1983. Theoretical and experimental study of fabrics developed by different shaped markers in two-dimensional simple shear. *Bull. Soc. géol. Fr., 7 Ser.*, **XXV**, 319–326.

Flinn, D. 1962. On folding during three-dimensional progressive deformation. *Q. Jl geol. Soc. Lond.* **68**, 385–433.

Gay, N. C. 1966. Orientation of mineral lineation along the flow direction in rocks: a discussion. *Tectonophysics* **3**, 559–564.

Gay, N. C. 1968. The motion of rigid particles in a viscous fluid during pure shear deformation of the fluid. *Tectonophysics* **5**, 81–88.

Hameurt, J. 1967. Les terrains cristallins et cristallophylliens du versant occidental des Vosges moyennes. *Mém. Serv. Carte géol. Als.-Lorr.* **26**.

Jeffery, G. B. 1922. The motion of ellipsoidal particles immersed in a viscous fluid. *Proc. R. Soc. Lond.* **A 102**, 161–179.

Johannes, W. & Gupta, L. N. 1982. Origin and evolution of a migmatite. *Contr. Miner. Petrol.* **79**, 114–123.

Johnson, A. M. & Pollard, D. D. 1973. Mechanics of growth of some laccolithic intrusions in the Henry Mountains, Utah. Field observations, Gilbert's model, physical properties and flow of the magma. *Tectonophysics* **18**, 261–309.

Lespinasse, M. & Mollier, B. 1985. Déformation magmatique et plastique en limite du granite de Saint-Sylvestre (Nord-Ouest du Massif Central français): la faille d'Arrènes-Ouzilly. *C.r. hebd. Séanc. Acad. Sci., Paris* **300**, 681–686.

Lister, G. S. & Snoke, W. A. 1984. S–C Mylonites. *J. Struct. Geol.* **6**, 617–638.

Mainprice, D., Bouchez, J. L., Blumenfeld, P. & Tubia, J. M. 1986. Dominant *c* slip in naturally deformed quartz: implications for dramatic plastic softening at high temperature. *Geology* **14**, 819–822.

March, A. 1932. Mathematische Theorie der Regelung nach der Korngestalt bei affiner Deformation. *Z. Kristallogr.* **81**, 285–297.

McLellan, E. L. 1983. Contrasting textures in metamorphic and anatectic migmatites: an example from the Scottish Caledonides. *J. metamorphic Geol.* **1**, 241–262.

Nicolas, A. & Poirier, P. 1976. *Crystalline Plasticity and Solid State Flow in Metamorphic Rocks*. Wiley, London.

Ramsay, J. G. 1980. Shear zone geometry: a review. *J. Struct. Geol.* **2**, 83–99.

Schoneveld, C. 1977. A Study of some typical inclusion patterns in

strongly paracrystalline-rotated garnets. *Tectonophysics* **39**, 453–471.

Simpson, C. & Schmid, S. M. 1983. An evaluation of criteria to deduce the sense of movement in sheared rocks. *Bull geol. Soc. Am.* **94**, 1281–1288.

Van Der Molen, I. & Paterson, M. S. 1979. Experimental deformation of partially melted granite. *Contr. Miner. Petrol.* **59**, 299–318.

Vernon, R. H. 1987. A microstructural indicator of shear sense in volcanic rocks and its relationship to porphyroblast rotation in metamorphic rocks. *J. Geol.* **95**, 127–133.

Willis, D. G. 1977. A kinematic model of preferred orientation. *Bull. geol. Soc. Am.* **88**, 883–894.

Winkler, H. G. F. 1979. *Petrogenesis of Metamorphic Rocks*. Springer Verlag, New York.